Photo- and solvatochromic properties of nitrobenzospiropyran in ionic liquids containing the $[NTf_2]^-$ anion†

Robert Byrne,[a] Kevin J. Fraser,[b] Ekaterina Izgorodina,[b] Douglas R. MacFarlane,[b] Maria Forsyth[c] and Dermot Diamond*[a]

Received 18th April 2008, Accepted 25th June 2008
First published as an Advance Article on the web
DOI: 10.1039/b806641h

The photo-, thermo- and solvatochromic properties of 2,3-dihydro-1′,3′,3′-trimethyl-6-nitrospiro-[1-benzopyran-2,2′-1H-indole] ($BSP-NO_2$) were studied in ILs containing the anion $[NTf_2]^-$ by UV-Vis absorption spectroscopy, *ab initio* molecular orbital theory and density functional theory (DFT) calculations. It was found that the kinetics and thermodynamics of the $BSP-NO_2 \leftrightarrow MC$ (merocyanine) equilibrium was sensitive to the nature of the cation. It was also observed that the imidazolium cation can form a through-space orbital interaction with the MC isomer, rather than a simple electrostatic interaction, thus preventing the MC conversion back to the $BSP-NO_2$ isomer. The $BSP-NO_2 \leftrightarrow MC$ equilibrium thus serves as a model system for studying modes of interaction of the cations in ionic liquids.

Introduction

Interest in the photo- and thermochromic effects in benzospiropyran (BSP, see Fig. 1), has gained much renewed attention over the last decade due to its unique properties and transformations.[1] BSP can exist in two thermodynamically stable states and is capable of interconversion between the two states under various external stimuli. This ability to reversibly switch the molecular form has led to great interest for applications such as light-sensitive eyewear,[2] information recording and processing,[3] optical memory,[4] molecular devices[5,6] and optical sensing.[7–9]

BSP consists of two heterocyclic moieties linked together by a common tetrahedral sp^3 carbon atom. The two halves of the molecule are in two orthogonal planes (A and B, Fig. 1). The benzopyran part (B) is the common structure to all spiropyran compounds, and the heterocyclic part (A) is built upon a benzofused azaheterocycle. BSP undergoes a heterocyclic ring cleavage at the C–O spiro bond that results in the formation of a planar, zwitterionic and highly conjugated chromophore that absorbs strongly in the visible region, this being the merocyanine isomer (MC).

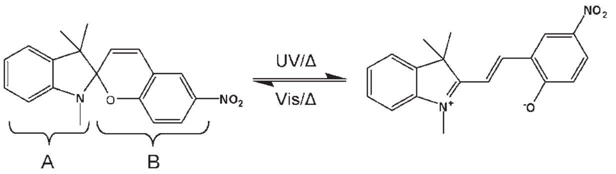

Fig. 1 Reversible photo- and thermochromic interconversion between nitrobenzospiropyran ($BSP-NO_2$, left) and merocyanine isomer (MC, right).

Like other merocyanines, the MC is a negative solvatochromic dye,[1] *i.e.* with increasing solvent polarity the absorption band undergoes a hypsochromic (or blue) shift. The effect of the solvent on the electronic spectra has been investigated previously and it has been shown that when the absorption maxima of MC (expressed in wavenumbers) or the transition energies are plotted against solvent polarity parameters such as $E_T(30)$ values,[10] Kosower's Z values,[11] Brooker's X_b values[12] and Brownstein's values,[13] reasonably linear plots are obtained. In addition to the solvatochromic effect, it has also been shown that changes in the absorption maxima, the intramolecular Lewis acid–base equilibrium between $BSP-NO_2$ and MC, and the thermal relaxation rates of MC back to $BSP-NO_2$, are intrinsically solvent-dependent.[14] Furthermore, the MC isomer has a phenolate anion site through which certain (d- and f-element) metal ions can bind, giving rise to a new absorption band in the visible spectrum. The type of metal ion only slightly influences the spectral properties of the complexes, in contrast to the relaxation time which can differ by one order of magnitude.[15] Thus, metal ion coordination can influence the photochromic properties of $BSP-NO_2$.

Ionic liquids (ILs) are a class of novel solvents with very interesting properties which are attracting the attention of a growing number of scientists and engineers, as shown by the increasing number of publications in recent years.[16] ILs are organic salts composed of anions and cations that are in the liquid state at ambient conditions and many show negligible volatility and non-flammability.[17] Hence, they are being actively investigated as alternative solvent media in synthesis,[18] catalysis,[19] polymerization,[20–22] separation,[23] electrochemistry[24,25] and electrochemical devices.[26,27] However, the basic science involved with fully characterizing these ILs is still in its

---

[a] *Adaptive Sensors Group, National Centre for Sensor Research, School of Chemical Sciences, Dublin City University, Dublin 9, Ireland*
[b] *School of Chemistry, Monash University, Clayton, 3800Victoria, Australia*
[c] *ARC Centre of Nanostructured Electromaterials, School of Physics and Materials Engineering, Monash University, Clayton, 3800Victoria, Australia*

† Electronic supplementary information (ESI) available: Fig. S1, showing the correlation between K_e and $E_T(30)$ values in molecular solvents and ionic liquids. See DOI: 10.1039/b806641h

infancy, and this may be holding back the complete and most efficient utilization of these *potentially*, and only in some cases,[28] "green" solvents. Before the full potential of ILs as solvent systems can be explored, more information about their physicochemical properties needs to be gathered. A number of fundamental physicochemical studies have already been published on ILs[29–33] ranging from the empirical determination of polarity utilizing the solvatochromic pyridinium *N*-phenolate betaine dye,[34,35] picosecond time-resolved fluorescence of 2-aminoquinoline[36] to the photoisomerization of 3,3′-diethyloxadicarbocyanine iodide[37] and 4′,7-dihydroxyflavylium[38] have been used to understand the many specific (*e.g.* hydrogen-bond donor and/or acceptor interactions) and non-specific interactions (*e.g.* Coulomb and Debye forces) within the ionic liquid. ILs can replace molecular solvents only if the chemist is able to compare ILs with generally used reaction media in a rational way; however, much further information is needed to allow the categorization of new and existing ILs more precisely in terms of solvent properties.

In this work we have investigated the spectroscopic properties of BSP-NO_2 in a number of bis(trifluoromethanesulfonyl) amide, $[NTf_2]^-$, ionic liquids. At the outset, the goal was to use this probe molecule to learn more about the modes of interaction and polarity of a number of the cations used in common ionic liquids. In the process some unusual BSP-NO_2 spectroscopic effects have been observed that may be of interest in the various applications discussed above.

Experimental

2,3-Dihydro-1′,3′,3′-trimethyl-6-nitrospiro-[1-benzopyran-2,2′-1H-indole] (BSP-NO_2) was purchased from Aldrich and used as received. Acetonitrile was HPLC grade and used without further purification. The phosphonium IL $[P_{6,6,6,14}][NTf_2]$ and ammonium IL $[Oct_3NMe][NTf_2]$ were supplied by Cytec industries and Merck respectively. $[C_3mpyr][NTf_2]$, $[C_4mpyr][NTf_2]$, $[emim][NTf_2]$ and $[edmim][NTf_2]$ were synthesized as described previously.[39,40] All ILs, Fig. 2, were purified thoroughly by column chromatography,[41] dried under vacuum at 40 °C for 48 h, and stored under argon at 20 °C before analysis. Absorption spectra were recorded on a Varian Cary 100 Bio UV-Visible Spectrophotometer, this instrument is also equipped with a temperature-controlled 6 × 6 multicell holder. The ultraviolet irradiation source was a Spectroline ENF-24OC/FE UV-365 nm obtained from Spectronics Corporation. The white light source was a Leica CLS 150×, 150 W obtained from Leica Microsystems. Samples were irradiated at a distance of 7 cm in a quartz cuvette. To determine the equilibrium constant K_e between BSP-NO_2 and MC in the various solvents, standard solutions of BSP were made up to 10^{-3} M in acetonitrile. 1 ml of this solution was placed in a vial and the solvent removed by N_2 stream. To this 10 ml of the selected IL (Fig. 2) was added to the vial and placed in sonicator for 20 minutes at 20 °C. Samples were stored under argon in the dark at 20 °C for 15 h before the absorbance measurement was taken.

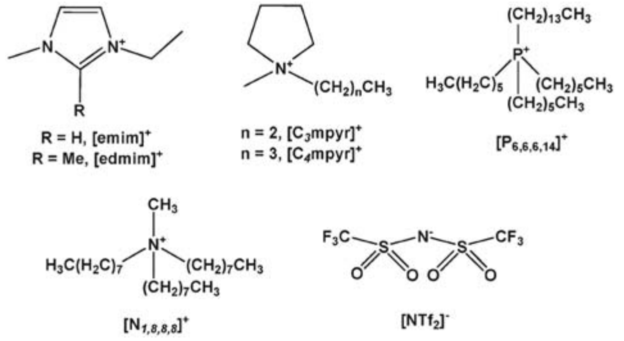

Fig. 2 Cations and anion used in this study: ethylmethylimidazolium $[emim]^+$, ethyldimethylimidazolium $[edmim]^+$, *N*-propyl-*N*-methylpyrrolidium $[C_3mpyr]^+$, *N*-butyl-*N*-methylpyrrolidium $[C_4mpyr]^+$, trihexyltetradecylphosphonium $[P_{6,6,6,14}]^+$, trioctylmethylammonium $[N_{1,8,8,8}]^+$ and bis(trifluoromethanesulfonyl)amide $[NTf_2]^-$.

Results

The physical properties of BSP-NO_2 in solution are determined by the ground-state equilibrium (Fig. 1) between the BSP-NO_2 form and the MC form. The absorption spectrum of BSP-NO_2 in acetonitrile at room temperature has two major bands with maxima in the UV and the visible. It is accepted that BSP-NO_2 in acetonitrile at room temperature has maxima at λ_{BSP} = 336 nm ($\varepsilon_{BSP} = 0.8 \times 10^4$ M^{-1} cm^{-1}) and λ_{MC} = 555 nm ($\varepsilon_{MC} = 3.5 \times 10^4$ M^{-1} cm^{-1}).[14] This data is well documented and for the results discussed herein, the properties of BSP-NO_2 in acetonitrile are used as point of reference. To support and validate our experimental results, the solvatochromic probe Reichardt's dye 30 has been used as a solvent-dependent reference process to define empirically a solvent polarity scale, called the $E_T(30)$ scale.

In determining the equilibrium constants K_e between BSP-NO_2 and MC in these ILs, it was required that the samples were kept in the dark at 20 °C for 15 h to reach equilibrium. At equilibrium, from Beer's law, we have

$$K_e = \frac{[MC]}{[BSP]} = \frac{A}{3.5 \times 10^4 \times C - A} \qquad (1)$$

where K_e is the equilibrium constant between BSP-NO_2 and MC, A is the equilibrium absorbance at the absorption maximum, C is the total concentration of BSP-NO_2 initially dissolved and $\varepsilon_{MC} = 3.5 \times 10^4$ M^{-1} cm^{-1} for the MC form of BSP-NO_2 according to Flannery.[42]

This thermal equilibrium between the BSP-NO_2 and MC is affected by the change in solvent polarity; polar solvents promote the formation of the coloured (MC) form and non-polar solvents promote the formation of the colourless (BSP-NO_2) form. This relationship is reinforced by plotting the K_e value *vs.* $E_T(30)$ values in the corresponding molecular solvents and achieving good linearity.[14] The correlation between the π–π* transition energies of the MC isomer and $E_T(30)$ implies the contributions of different solute–solvent interactions, as measured by Reichardt's dye 30, are nearly the same as for the π–π* absorptions of MC. Therefore, transition energies of the MC isomer can be used to measure micropolarity of a solvent on the molecular level.

The experimental K_e values (Table 1) for the pyrrolidium based ILs, $[C_3mpyr]^+$ and $[C_4mpyr]^+$, are quite similar and

Table 1 Equilibrium and photo-physical constants of BSP-NO_2 and $E_T(30)$ values of various molecular solvent and ionic liquids. (BSP-NO_2 and Reichardt's dye 30 concentration 10^{-4} M)

Solvent	λ_{max} for MC/nm	$A_e{}^a$ Q8	$K_e \times 10^{-2b}$	$k \times 10^{-2}/s^{-1c}$	$E_T(30)$/kcal mol^{-1}
Acetonitrile	554	0.13	3.85	8.8	45.5 (45.6)[43]
Ethanol	539	0.15	4.57	1.9	51.8 (51.9)[43]
Dichloromethane	578	0.01	0.51	70.0	40.6 (40.7)[43]
$[C_3mpyr][NTf_2]$	549	0.14	4.16	6.9	48.9
$[C_4mpyr][NTf_2]$	551	0.13	3.85	7.8	48.1 (48.3)[32]
$[P_{6,6,6,14}][NTf_2]$	574	0.04	1.15	8.5	47.97
$[emim][NTf_2]$	544	0.15	4.57	2.1	53.3 (53.1)[35]
$[edmim][NTf_2]$	548	0.11	3.24	3.9	51.79
$[N_{1,8,8,8}][NTf_2]$	550	0.14	4.16	4.0	49.13

[a] Absorbance measured at λ_{max} for MC after 15 h in dark. [b] Calculated from eqn (1). [c] Thermal relaxation rate constant calculated by eqn (2) after 60 s of 360 nm light. [d] $E_T(30)$ values in parenthesis are from the literature.

represent values expected for polar aprotic molecular solvents such as acetonitrile. On comparison with the $E_T(30)$ scale pyrrolidium-based ILs appear more polar than acetonitrile. K_e values for the imidazolium based ILs, $[emim]^+$ and $[edmim]^+$, correspond to polar protic and aprotic molecular solvents respectively. The imidazolium-based IL $[edmim]^+$ has value similar to those of primary alcohols whereas $[emim]^+$ appears more polar (similar to an alcohol-based binary solvent containing water) on the $E_T(30)$ scale. The quaternary tetra-alkylammonium-based $[N_{1,8,8,8}]^+$ and -phosphonium-based $[P_{6,6,6,14}]^+$ ILs exhibit K_e values typical of polar aprotic solvents, while their respective $E_T(30)$ values are classed as aliphatic alcohols. A Figure representing the correlation between the K_e and $E_T(30)$ values in each solvent studied can be found in the electronic supplementary information (Fig. S1, ESI).†

It has been previously reported that a direct relationship can be observed between the equilibrium constant K_e and the solvatochromic visible absorption shift of BSP-NO_2; as K_e decreases the λ_{max} shifts towards longer wavelengths. This trend is also seen in the ILs studied herein: for $[emim]^+$ the MC $\lambda_{max} = 544$ nm and $K_e = 4.47 \times 10^{-2}$, whereas $[P_{6,6,6,14}]^+$ exhibits an MC $\lambda_{max} = 574$ nm and $K_e = 1.15 \times 10^{-2}$. Thus, the MC λ_{max} of the $[P_{6,6,6,14}]^+$-based IL is red-shifted by 20–30 nm compared with the rest of the ILs, although its $E_T(30)$ value is higher than that of acetonitrile (MC $\lambda_{max} = 554$ nm). Dichloromethane has a similar MC λ_{max} to $[P_{6,6,6,14}]^+$ but its $E_T(30)$ value is significantly lower. Solvatochromic shifts of the MC isomer in ILs are listed in Table 1.

The equilibrium between BSP-NO_2 and MC is strongly displaced upon irradiation with visible (≥ 450 nm) light towards the BSP-NO_2 isomer and when irradiated with UV light (360 nm) towards the MC isomer. Fig. 3 displays the resulting spectra of selected ILs after 60 s of UV irradiation. The effect of visible irradiation is shown for comparison (spectrum $[C_3mpyr]^+$-Vis) to show the significant difference between the MC and BSP-NO_2 spectra. It is well known that, after removal of UV light, the predominant MC form generated will thermally isomerize back to its equilibrium state (K_e); this decay in absorbance should follow first-order kinetics[44] as it does in molecular solvents. The rate at which the thermal isomerization occurs is strongly solvent-dependent.

$$y = ae^{-kt} + b \qquad (2)$$

First-order rate constants for the thermal isomerization were determined in this work using Microsoft Excel Solver, by fitting the absorbance data to eqn (2), where y is the absorbance value at the λ_{max}, a is the absorbance at $t = 0$, k is the rate constant, t is time and b is asymptotic value.[45] The rate constants for MC thermal isomerization in the selected ILs are tabulated in Table 1.

$[C_3mpyr]^+$ and $[C_4mpyr]^+$ exhibit similar rate constants to acetonitrile at their respective MC maxima, whereas $[emim]^+$, $[edmim]^+$ and $[N_{1,8,8,8}]^+$ exhibit much slower thermal reversion to BSP-NO_2 with rate constants that are broadly similar to those exhibited by protic molecular solvents, such as ethanol under similar conditions.[44,46] From the K_e values and λ_{max} positions in Table 1, it would be expected that the $[P_{6,6,6,14}]^+$ IL should exhibit the largest rate constant; this hypothesis proved to be correct, the rate constant for $[P_{6,6,6,14}]^+$ being 4 times faster than that of $[emim]^+$. However, comparing $[P_{6,6,6,14}]^+$ with dichloromethane, whose λ_{max} position is quite similar, their rate constants differ by nearly an order of magnitude. These observations raise some interesting issues about solute–solvent interactions within ILs. These questions are investigated further below by means of *ab initio* theoretical calculations.

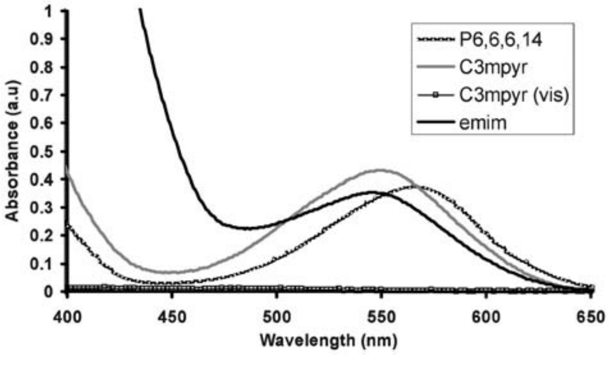

Fig. 3 $[P_{6,6,6,14}]$, $[C_3mpyr]^+$ and $[emim]^+$ $[NTf_2]^-$ IL solutions of BSP-NO_2 exposed to 60 s irradiation at 365 nm. $[C_3mpyr]^+$ IL solution of BSP-NO_2 exposed to 60 s irradiation of visible light (≥ 450 nm). Q9

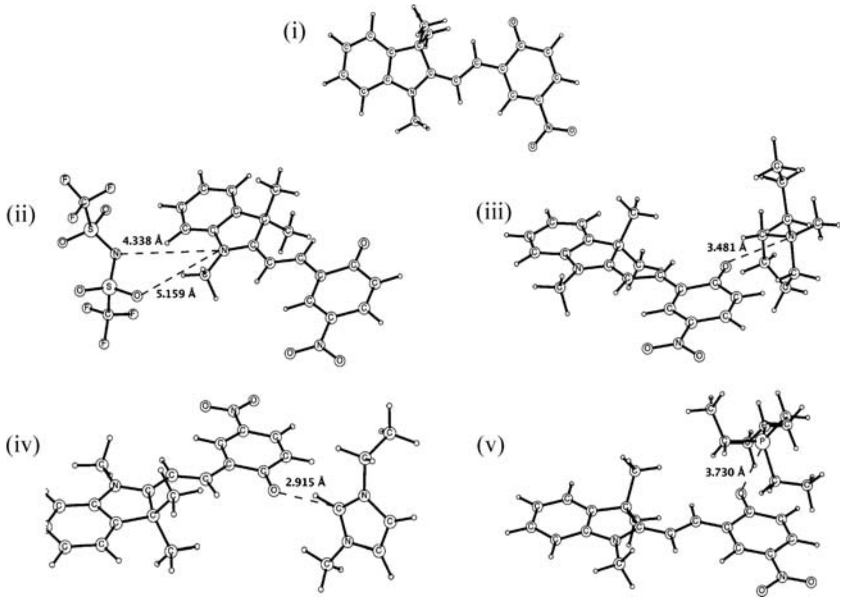

Fig. 4 Optimized structures of (i) MC isomer together with the complexes that can be formed with (ii) $[NTf_2]^-$, (iii) $[C_3mpyr]^+$, (iv) $[emim]^+$, (v) $[P_{2,2,2,2}]^+$ at B3LYP/6-31 + G(d).

Ab initio calculations

Standard *ab initio* molecular orbital theory and density functional theory (DFT) calculations were carried out using GAUSSIAN 03.[47] The MC isomer together with $[emim]^+$, $[C_3mpyr]^+$, $[P_{6,6,6,14}]^+$ and $[NTf_2]^-$ were optimized at B3LYP/6-31 + G(d) level of theory. As the optimization for the $[P_{6,6,6,14}]^+$ cation was not feasible, a model cation, $[P_{2,2,2,2}]^+$, was used instead. It is important to note that these calculations represent descriptions of the gas-phase molecules and complexes only. However, the ability of gas-phase calculations to estimate the real *n*–π* and π– π* electronic transition energies in organic molecules has been demonstrated previously.[48] The optimized geometries are shown in Fig. 4. The excitation energies of the MC isomer were computed at CIS(D)/6-31 + G(d,p) level. All molecular orbitals were plotted using the HF/6-31 + G(d,p) electron density.

Discussion

From the spectroscopic results obtained, we see that the ILs containing the ions $[C_3mpyr]^+$ and $[C_4mpyr]^+$ together with $[NTf_2]^-$ have no profound effect on the BSP-NO_2 spectroscopy, only a solvatochromic effect similar to that of the molecular solvent acetonitrile. For discussion purposes, the pyrrolidium-based ILs shall be used as a point of reference when discussing cation effects; any cation that interacts more strongly than these will have a more profound effect on the spectroscopic properties of BSP-NO_2. The ILs containing the cations $[emim]^+$ and $[P_{6,6,6,14}]^+$ exhibit the greatest difference in MC spectroscopic characteristics and we focus on the intermolecular interactions that cause these differences. Since we are observing changes in spectroscopy of the planar MC isomer, it is important to investigate its excitation energies. The molecular orbitals on the MC isomer are shown in Fig. 5. The first excitation arising from the HOMO has energy of 569 nm; this excitation is allowed by symmetry and is seen in the visible spectrum.

Molecular orbital calculations for the gas-phase complexes show that the anion resides approximately 4.3 Å from the positively charged MC nitrogen, hence the anion $[NTf_2]^-$ may only weakly polarize the molecular system. This distance is comparable with that found in the pure $[C_1mpyr][NTf_2]$ plastic crystal, in which the N···N separation lies in the range of 4.5 and 6.3 Å.[49] Thus the anion does not appreciably interact with the

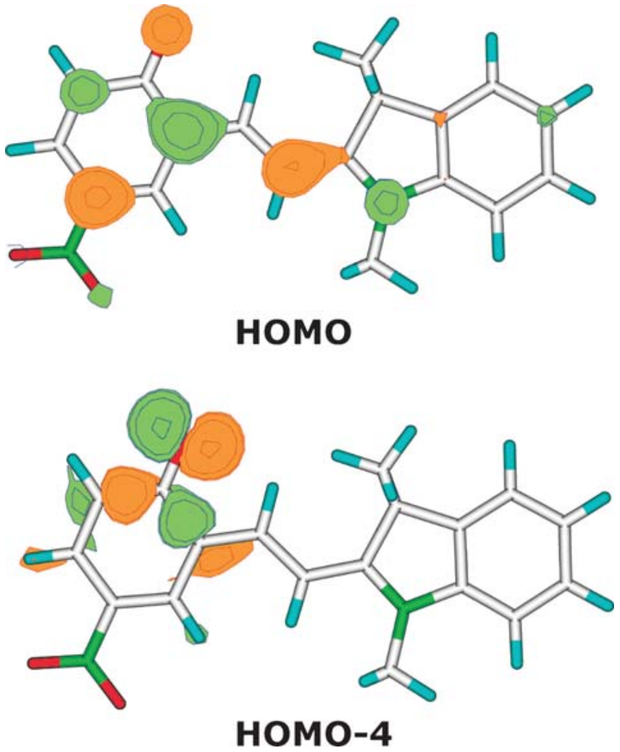

Fig. 5 HOMO and HOMO-4 molecular orbitals of the MC isomer.

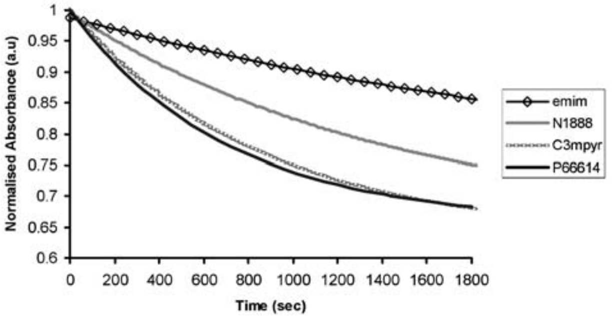

Fig. 6 First-order kinetic plot of the thermal relaxation of the MC isomer in selected ILs after 60 s UV irradiation. Data normalized at 1.0 a.u.

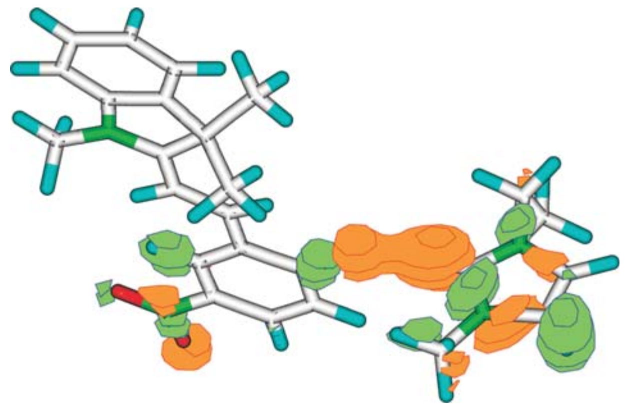

Fig. 7 Molecular orbital of the [emim]$^+$[MC] complex showing a through-space interaction between the phenolate oxygen and the carbon atom (the C$_2$ position) on [emim]$^+$.

positively charged nitrogen on the MC and is not expected to influence the spectroscopy beyond a possible solvatochromic effect. As [NTf$_2$]$^-$ is the anion in all of the ILs studied, the difference in spectroscopy observed is therefore a result of the different cations. In the case of the [C$_3$mpyr]$^+$ cation, the pyrrolidinium nitrogen is positioned approximately 3.5 Å away from the phenolate oxygen; in this case the sum of the van der Waals radii of N and O is 3.07 A and thus this is not a close contact.

[P$_{6,6,6,14}$]$^+$ was also found to behave differently from [C$_3$mpyr]$^+$; from the spectroscopy it is evident that the BSP-NO$_2$ isomer is preferred over the MC isomer at equilibrium. Also, after UV irradiation the MC isomer $\lambda_{\max}$ indicates the molecule to be in a non-polar environment, furthermore the thermal kinetics is faster than that of [C$_3$mpyr]$^+$. This can be explained by geometry optimization on the model phosphonium cation, [P$_{2,2,2,2}$]$^+$, which shows that the cation resides 3.73 Å from the phenolate oxygen, this interaction distance being larger by 0.25 Å than that for [C$_3$mpyr]$^+$. The cation does not appreciably interact with the positively charged nitrogen on the MC and is not expected to influence the spectroscopy beyond a possible solvatochromic effect. According to the spectroscopic analysis, [emim]$^+$ was found to behave differently than the pyrrolidinium cations, having a larger K_e value and thermal kinetics more than three times slower (Fig. 6). Fig. 3 shows the spectrum of the MC isomer after 60 s UV irradiation; it can be clearly seen that in the [emim]$^+$ IL it absorbs very strongly after 440 nm compared to the rest of the ILs. This might be understood on the basis of the MC isomer's molecular orbital shown in Fig. 5. An excitation arising from HOMO-4 (the π orbital on the phenolate oxygen) has predicted energy of 418 nm; this is not seen in experiments since the transition is forbidden due to the symmetry of this orbital, the oscillator strength being zero. However, should the symmetry of this transition be altered through interactions with cations and/or polarization by cations, the transition may be seen in the absorption spectrum, as is the case for transition metal ions.[50] Thus this transition may be responsible for the 440 nm band observed, if an interaction with the phenolate oxygen and the cation are sufficiently strong.

The [emim]$^+$ cation appears to interact predominantly *via* the C2 carbon which resides only 2.92 Å (the C$\cdots$O distance, Fig. 4) away from the phenolate oxygen. The sum of the van der Waals radii of the carbon and oxygen atoms is 3.22 Å and hence, the C$\cdots$O separation appears to be considerably shorter than a normal close contact. This C2 hydrogen is in fact known to be quite acidic.[51] The C2 hydrogen atom sits in between the carbon and oxygen atoms (CHO bond angle close to linear) introducing a very short/strong hydrogen bond of just 1.865 Å (H–O distance). As a comparison, a strong hydrogen bond, *e.g.* O–H$\cdots$O, is slightly longer in length, around 1.9 Å.[52] Moreover, such a close proximity of the two ions results in a through-space orbital interaction, with molecular orbitals on both oxygen and carbon atoms overlapping (Fig. 7) thus forming a strong interaction between the two molecules. The possibility of complete proton transfer was ruled out by comparing the pK_a values of phenol (pK_a = 10) and the unsubstituted imidazolium cation (pK_a = 23).[53] Due to the through-space interaction, the species formed is likely to be quite stable and will thus hinder conversion of the MC form back to the aplanar isomer. To emphasize the effect of the C2 position, we see that the [edmim]$^+$ cation, which bears a methyl group at the C2 position, exhibits kinetics twice as fast as the [emim]$^+$ cation (Table 1).

The through-space interaction will have a polarizing effect on the MC moeity, disrupting the symmetry of the π orbital on the phenolate and allowing the π–π* transition of the MC at calculated excitation energy of 418 nm. This accords with the spectroscopic results, accounting for absorption at 440 nm and thus supports the hypothesis that [emim]$^+$ forms a stable complex with MC.

Conclusions

To our knowledge this is the first demonstration of photochromic behavior of nitrobenzospiropyran in the mentioned ionic liquid solvents and that the kinetics and thermodynamics of the process are sensitive to the nature of the cation. It was also observed that the imidazolium cation can form a through-space orbital interaction rather than just electrostatic interactions, thus preventing the MC conversion back to the aplanar isomer. In conclusion, we have demonstrated that, in principle, we can optically switch the cation binding to the merocyanine on/off. We regard these preliminary results as pointing the way towards more sophisticated materials capable of switching reversibly between two distinct forms, and simultaneously providing a number of transduction modes for gathering information about the molecular environment in the immediate vicinity of the binding site and its surrounding environment.

Acknowledgements

RB wishes to thank Science Foundation Ireland for grant support for this research under the Adaptive Information Cluster Award (SFI 03/IN3/1361). EII gratefully acknowledges generous allocations of the computing time at the National Facility of the Australian Partnership for Advanced Computing.

References

1 V. I. Minkin, *Chem. Rev.*, 2004, **104**, 2751–2776.
2 J. C. Crano, T. Flood, D. Knowles, A. Kumar and B. Van Gemert, *Pure Appl. Chem.*, 1996, **68**, 1395–1398.
3 R. Guglielmetti, *Stud. Org. Chem.*, 1990, **40**, 855–878.
4 A. S. Dvornikov, J. Malkin and P. M. Rentzepis, *J. Phys. Chem.*, 1994, **98**, 6746–6752.
5 T. Yoshida and A. Morinaka, *J. Photochem. Photobiol., A*, 1994, **78**, 179–183.
6 I. Willner, S. Rubin, R. Shatzmiller and T. Zor, *J. Am. Chem. Soc.*, 1993, **115**, 8690–8694.
7 R. J. Byrne, S. E. Stitzel and D. Diamond, *J. Mater. Chem.*, 2006, **16**, 1332–1337.
8 S. Stitzel, R. Byrne and D. Diamond, *J. Mater. Sci.*, 2006, **41**, 5841–5844.
9 R. Byrne and D. Diamond, *Nat. Mater.*, 2006, **5**, 421–424.
10 C. J. Drummond and D. N. Furlong, *J. Chem. Soc., Faraday Trans.*, 1990, **86**, 3613–3621.
11 E. M. Kosower, *J. Am. Chem. Soc.*, 1958, **80**, 3253–3260.
12 L. G. S. Brooker, A. C. Craig, D. W. Heseltine, P. W. Jenkins and L. L. Lincoln, *J. Am. Chem. Soc.*, 1965, **87**, 2443–2450.
13 S. Brownstein, *Can. J. Chem.*, 1960, **38**, 1590–1596.
14 X. Song, J. Zhou, Y. Li and Y. Tang, *J. Photochem. Photobiol., A*, 1995, **92**, 99–103.
15 H. Gorner and A. K. Chibisov, *J. Chem. Soc., Faraday Trans.*, 1998, **94**, 2557–2564.
16 *Ionic Liquids: Industrial Applications for Green Chemistry*, ed. R. D. Rogers and K. R. Seddon, Proceedings of a Symposium held 1–5 April 2001 in San Diego, California, 2002 [*ACS Symp. Ser.*, 2002, 818].
17 S. A. Forsyth, J. M. Pringle and D. R. MacFarlane, *Aust. J. Chem.*, 2004, **57**, 113–119.
Q12 18 P. Wasserscheid, *Org. Synth. Highlights V*, 2003, 105–117.
19 G. A. Olah, T. Mathew, A. Goeppert, B. Toeroek, I. Bucsi, X.-Y. Li, Q. Wang, E. R. Marinez, P. Batamack, R. Aniszfeld and G. K. S. Prakash, *J. Am. Chem. Soc.*, 2005, **127**, 5964–5969.
20 C. Hardacre, J. D. Holbrey, S. P. Katdare and K. R. Seddon, *Green Chem.*, 2002, **4**, 143–146.
21 R. Vijayaraghavan and D. R. MacFarlane, *Chem. Commun.*, 2004, 700–701.
22 R. Vijayaraghavan and D. R. MacFarlane, *Aust. J. Chem.*, 2004, **57**, 129–133.
23 K. E. Gutowski, G. A. Broker, H. D. Willauer, J. G. Huddleston, R. P. Swatloski, J. D. Holbrey and R. D. Rogers, *J. Am. Chem. Soc.*, 2003, **125**, 6632–6633.
24 A. I. Bhatt, I. May, V. A. Volkovich, M. E. Hetherington, B. Lewin, R. C. Thied and N. Ertok, *J. Chem. Soc., Dalton Trans.*, 2002, 4532–4534.
25 J. M. Pringle, M. Forsyth, G. G. Wallace and D. R. MacFarlane, *Macromolecules*, 2006, **39**, 7193–7195.
26 W. Lu, A. G. Fadeev, B. Qi, E. Smela, B. R. Mattes, J. Ding, G. M. Spinks, J. Mazurkiewicz, D. Zhou, G. G. Wallace, D. R. MacFarlane, S. A. Forsyth and M. Forsyth, *Science*, 2002, **297**, 983–987.
27 P. C. Howlett, D. R. MacFarlane and A. F. Hollenkamp, *Electrochem. Solid-State Lett.*, 2004, **7**, A97–A101.
28 D. R. MacFarlane and K. R. Seddon, *Aust. J. Chem.*, 2007, **60**, 3–5.
29 C. Chiappe and D. Pieraccini, *J. Phys. Org. Chem.*, 2005, **18**, 275–297.
30 P. K. Mandal, A. Paul and A. Samanta, *J. Photochem. Photobiol., A*, 2006, **182**, 113–120.
31 R. E. Del Sesto, G. A. Baker, S. N. Baker, B. L. Scott, T. S. Keizer, A. K. Burrell and T. M. McCleskey, *Chem. Commun.*, 2006, 272–274.
32 L. Crowhurst, P. R. Mawdsley, J. M. Perez-Arlandis, P. A. Salter and T. Welton, *Phys. Chem. Chem. Phys.*, 2003, **5**, 2790–2794.
33 S. Arzhantsev, H. Jin, G. A. Baker and M. Maroncelli, *J. Phys. Chem. B*, 2007, **111**, 4978–4989.
34 K. A. Fletcher, I. A. Storey, A. E. Hendricks, S. Pandey and S. Pandey, *Green Chem.*, 2001, **3**, 210–215.
35 C. Reichardt, *Green Chem.*, 2005, **7**, 339–351.
36 K. Iwata, M. Kakita and H.-O. Hamaguchi, *J. Phys. Chem. B*, 2007, **111**, 4914–4919.
37 D. Chakrabarty, A. Chakraborty, P. Hazra, D. Seth and N. Sarkar, *Chem. Phys. Lett.*, 2004, **397**, 216–221.
38 F. Pina, A. J. Parola, M. J. Melo, C. A. T. Laia and C. A. M. Afonso, *Chem. Commun.*, 2007, 1608–1610.
39 D. R. MacFarlane, P. Meakin, J. Sun, N. Amini and M. Forsyth, *J. Phys. Chem. B*, 1999, **103**, 4164–4170.
40 T. De Diego, P. Lozano, S. Gmouh, M. Vaultier and J. L. Iborra, *Biotechnol. Bioeng.*, 2004, **88**, 916–924.
41 M. J. Earle, C. M. Gordon, N. V. Plechkova, K. R. Seddon and T. Welton, *Anal. Chem.*, 2007, **79**, 758–764.
42 J. B. Flannery, Jr, *J. Am. Chem. Soc.*, 1968, **90**, 5660–5671.
43 C. Reichardt, *Chem. Rev.*, 1994, **94**, 2319–2358.
44 H. Gorner, *Phys. Chem. Chem. Phys.*, 2001, **3**, 416–423.
45 D. Diamond and V. C. A. Hanratty, *Spreadsheet Applications in Chemistry Using Microsoft Excel*, Wiley, 1997. Q13
46 G. Sciaini, D. E. Wetzler, J. Alvarez, R. Fernandez-Prini and M. Laura Japas, *J. Photochem. Photobiol., A*, 2002, **153**, 25–31.
47 M. J. Frisch, G. W. Trucks, H. B. Schlegel, G. E. Scuseria, M. A. Robb, J. R. Cheeseman, J. A. Montgomery, Jr., T. Vreven, K. N. Kudin, J. C. Burant, J. M. Millam, S. S. Iyengar, J. Tomasi, V. Barone, B. Mennucci, M. Cossi, G. Scalmani, N. Rega, G. A. Petersson, H. Nakatsuji, M. Hada, M. Ehara, K. Toyota, R. Fukuda, J. Hasegawa, M. Ishida, T. Nakajima, Y. Honda, O. Kitao, H. Nakai, M. Klene, X. Li, J. E. Knox, H. P. Hratchian, J. B. Cross, V. Bakken, C. Adamo, J. Jaramillo, R. Gomperts, R. E. Stratmann, O. Yazyev, A. J. Austin, R. Cammi, C. Pomelli, J. Ochterski, P. Y. Ayala, K. Morokuma, G. A. Voth, P. Salvador, J. J. Dannenberg, V. G. Zakrzewski, S. Dapprich, A. D. Daniels, M. C. Strain, O. Farkas, D. K. Malick, A. D. Rabuck, K. Raghavachari, J. B. Foresman, J. V. Ortiz, Q. Cui, A. G. Baboul, S. Clifford, J. Cioslowski, B. B. Stefanov, G. Liu, A. Liashenko, P. Piskorz, I. Komaromi, R. L. Martin, D. J. Fox, T. Keith, M. A. Al-Laham, C. Y. Peng, A. Nanayakkara, M. Challacombe, P. M. W. Gill, B. G. Johnson, W. Chen, M. W. Wong, C. Gonzalez and J. A. Pople, *GAUSSIAN 03 (Revision C.02)*, Gaussian, Inc., Wallingford, CT, 2004. Q14
48 S. Grimme and E. I. Izgorodina, *Chem. Phys.*, 2004, **305**, 223–230.
49 C. M. Forsyth, D. R. MacFarlane, J. J. Golding, J. Huang, J. Sun and M. Forsyth, *Chem. Mater.*, 2002, **14**, 2103–2108.
50 H. Gorner and A. K. Chibisov, *J. Chem. Soc., Faraday Trans.*, 1998, **94**, 2557–2564.
51 D. R. MacFarlane, J. M. Pringle, K. M. Johansson, S. A. Forsyth and M. Forsyth, *Chem. Commun.*, 2006, 1905–1917.
52 K. Modig, B. G. Pfrommer and B. Halle, *Phys. Rev. Lett.*, 2003, **90**, 075502. Q15
53 A. M. Magill and B. F. Yates, *Aust. J. Chem.*, 2004, **57**, 1205–1210.

This journal is © the Owner Societies 2008